Time evolution of the local slope during Cu(110) ion sputtering

C. Boragno, F. Buatier, G. Costantini, A. Molle, D. de Sanctis, and U. Valbusa
INFM-UdR Genova, and Dipartimento di Fisica, Genova, Italy

F. Borgatti and R. Felici
INFM OGG-Grenoble, c/o ESRF, Grenoble, France

S. Ferrer
ESRF, Grenoble, France

(Received 13 November 2002; revised manuscript received 13 May 2003; published 3 September 2003)

The time evolution of the morphology of the Cu(110) surface during ion sputtering has been studied *in situ* and in real time by x-ray-based techniques. The surface was bombarded with Ar^+ ions at an energy of 1 keV in the temperature range 100–320 K; the ion incidence angle was set out of the x-ray scattering plane in order to induce asymmetric nanostructures. The results show that the ripples or mounds formed by the ion sputtering evolve in time, changing the spatial periodicity and the local slope of the facets. The latter is strongly dependent on temperature; moreover the facets along the $\langle 1-10\rangle$ direction evolve in a different way from those along $\langle 001\rangle$.

DOI: 10.1103/PhysRevB.68.094102 PACS number(s): 68.55.Jk, 68.37.−d, 61.10.−i

The possibility to nanopattern a nonmetallic surface by means of ion sputtering has been extensively studied in recent years, since this method offers a simple way to create periodic morphologies;[1–3] the method can have also technological relevance regarding the production of microelectronic devices, as demonstrated in Refs. 4 and 5. Generally, the structures are interpreted to be interface instabilities caused by sputtering erosion which competes with slow surface diffusion. Also in metals, regular structures can be produced,[6] but in this case surface atomic diffusion biased by an Ehrlich-Schwoebel barrier at descending steps might become the leading process responsible for the structure formation. The surface symmetry forces the resulting morphology, leading to hexagonal pits in Pt(111) (Ref. 7) and Au(111) (Ref. 8) or square holes in Ag (001) (Ref. 9) and Cu(001).[10,11] In the case of anisotropic surfaces, the asymmetry in surface diffusion induces the formation of characteristic ripplelike structures.[12]

The majority of these experiments have been done by scanning tunneling microscopy, a method which, however, does not allow to follow the evolution of the morphology *in real time*. x-ray diffraction overcomes this limitation, since data can be taken during the ion etching process.

In a recent experiment[13] we demonstrated that it is possible to measure by x ray the local slope and the periodicity of the nanostructures induced by ion sputtering in the case of Ag(110). In the present experiment, we apply the same method to Cu(110) but with a different scattering geometry: now the ion beam impinges on the surface in an asymmetric way, i.e., out of the plane determined by the surface normal and a principal surface direction ($\langle 100\rangle$ or $\langle 1-10\rangle$). Following the time evolution of the local slope along the two principal surface directions, we want to understand how the system develops until a well-defined slope is gained and if the sputtering geometry has some influence on the final morphology. We measured the time dependence of the forward scattering using grazing incidence small-angle x-ray scattering (GISAXS). The sample was also characterized by the measurement of the crystal truncation rods (CTR) for the two inequivalent high-symmetry surface directions. GISAXS spectra provide information on the correlation of surface density fluctuations and thus the long-range morphological order as reported in Ref. 14. CTR are due to the truncation of the lattice induced by the surface. They are always normal to the surface and their dependence on the vertical-momentum transfer gives information on the structural properties of terminating layers and allows the determination of the slope of the structure facets.[15]

Measurements were carried out at the ID03 beamline of the European Synchrotron Radiation Facility in Grenoble, France. This beamline is devoted to surface x-ray-diffraction measurements and is equipped with a large six-circle diffractometer coupled to a UHV chamber with a base pressure of about 1×10^{-10} mbar. [16] The sample holder is connected to a liquid-nitrogen flow cryostat to cool the sample down to a minimum of 120 °K. The sample was mounted on a boron nitride heater and the temperature was controlled by a thermocouple in contact with the sample. The accuracy of the sample temperature was ±5 K. The Cu(110) surface had a miscut from the nominal surface of less 0.1°. The surface was prepared by several cycles of sputtering and annealing at 750 K for 5 min, with the procedure repeated before each sputtering experiment. A Varian ion gun provided a constant Ar^+-ion current of 5 μA/cm^2, corresponding to an ion flux Φ of 0.015 ML/sec (1 ML$=8.44\times10^{14}$ ion/cm^2).

The Cu(110) surface is anisotropic in nature: close-packed rows of atoms run along $\langle 1-10\rangle$, whereas in the $\langle 001\rangle$ direction the interatomic distance is $\sqrt{2}$ times the nearest-neighbor distances. The unit cell is given by A_1, A_2, A_3 which are parallel to the $\langle 1-10\rangle$, $\langle 001\rangle$, and $\langle 110\rangle$ directions, respectively, with $A_1=A_3=0.2556$ nm, and $A_2=0.3615$ nm. The corresponding reciprocal-lattice directions are designed as H, K, and L, respectively. Bulk Bragg reflections are found at (H,K,L) values with $L=1,3,5,...$ or $L=0,2,4,...$, depend-

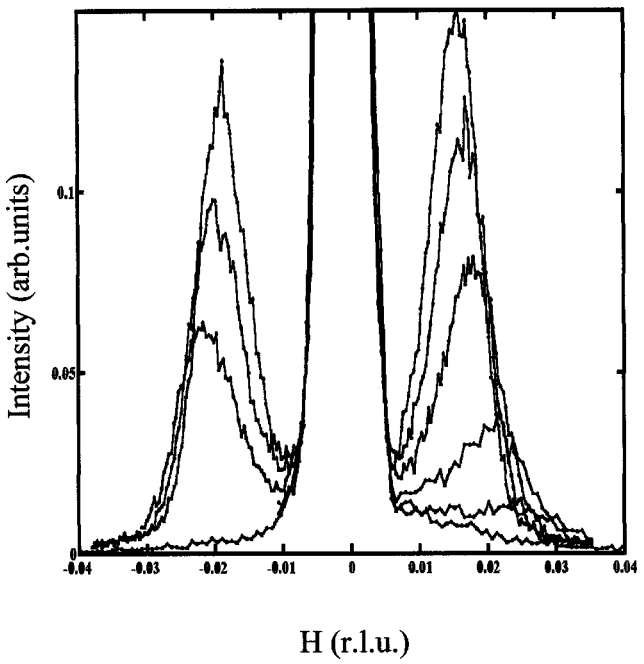

FIG. 1. Collection of scans acquired in GISAXS geometry at different sputtering times.

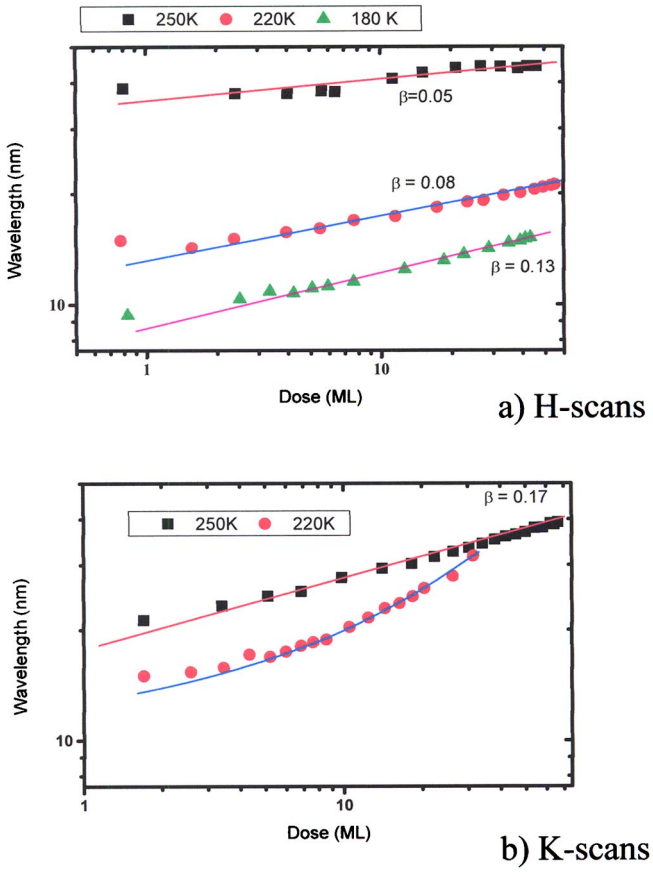

FIG. 2. Time evolution of the periodicity seen by an x-ray beam along the two principal directions: (a) *H* scans; (b) *K* scans. For *K* scans and *H* scans the detector is moved along the x-ray beam aligned along the $\langle 1-10\rangle$ or $\langle 001\rangle$ direction, respectively.

ing on whether **H** and **K** have the same or different parities. As is customary in surface x-ray diffraction, the **L** values denote the perpendicular momentum transfer and are continuously varying along the so-called crystal truncation rods.

With respect to a previous experiment on Ag(110),[13] we changed the sputtering geometry: the scattering plane of the x rays is defined by the surface normal and another principal surface direction ($\langle 100\rangle$ or $\langle 1-10\rangle$), but now the ion beam forms with it an angle γ of 23° and an angle $\delta=36°$ with respect to the surface normal. We have chosen this geometry in order to check if there is any effect of ion-beam alignment on the shape of the nanostructures induced on the surface. As described below, this geometrical arrangement of the ion beam changes the results significantly.

As a general overview of the results, we found that the system changes from a ripple morphology along the $\langle 100\rangle$ direction at lower T, to a mound structure at intermediate temperatures, to again reach a ripple structure along $\langle 1-10\rangle$ at higher T, in complete analogy to previous observations.[12,13] However, this experiment produced new information about the time evolution of the system and the local slopes under nonsymmetric sputtering conditions.

In Fig. 1 we show GISAXS spectra taken at 180 K. The spectra show the variation of the specular beam intensity at the (0 0 0.6) reciprocal-lattice point moving the detector along the $\langle 1-10\rangle$ direction, while the x-ray beam is aligned along the $\langle 100\rangle$ surface direction (in the following, we call these *H* scans). The spectra were collected continuously during sputtering with an acquisition time for a single scan of about 100 sec. Two side peaks which move towards the specular peak with sputter time are clearly resolved. From the position of the two peaks, it is possible to calculate the modulation period $\lambda=2\pi/q_p$ where q_p is the distance to the center of the satellite from the diffraction peak. The result of this analysis is shown in Fig. 2 for three different temperatures and for *H* scans and *K* scans (in *K* scans, the detector is moved along the $\langle 100\rangle$ direction, with the x-ray beam aligned along the $\langle 1-10\rangle$ direction).

At 180 K, only *H* scans show the satellite peaks, indicating the formation of ripples having the crests along the $\langle 100\rangle$ direction [in the following, we refer to this morphology as low-temperature ripples (LTR)]. Increasing the temperature, both *H* and *K* scans reveal lateral peaks, proving the formation of periodicity along the two directions and then the formation of mounds. We refer to this geometry as intermediate-temperature mounds (ITM). Along both directions, the spatial periodicity increases with temperature (by more than a factor of 4 for *H* scans); moreover, the wavelength increases with the ion dose $\Psi=\Phi t$ (t is the sputtering time) following a power law $\lambda\approx\Psi^{\beta}$, but β lowers with temperature: $\beta=0.13$, 0.08, and 0.05 for *H* scans at 180, 220, and 250 K, respectively. For *K* scans a power law is well defined only at $T=250$ K ($\beta=0.17$), but not at $T=220$ K. At higher temperatures, the high-temperature ripple (HTR) phase (i.e., ripples aligned along $\langle 1-10\rangle$) is present, but the instrument resolution was not sufficient to allow a quantitative analysis.

In order to follow in real time the evolution of the facet slope of the nanostructures, we recorded subsequent rocking

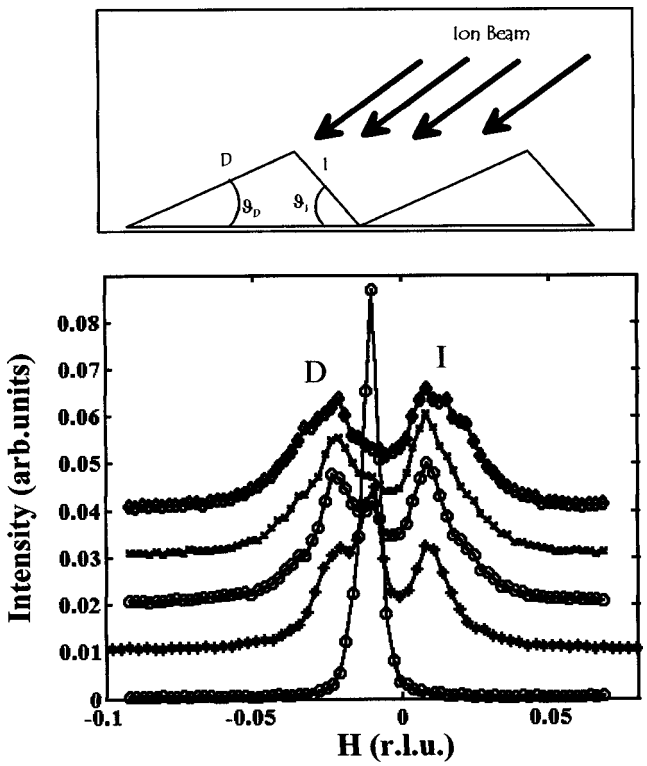

FIG. 3. Collection of scans acquired along the rocking curve at the (1 0 0.6) point in reciprocal space.

scans at the (1 0 0.6) or (0 1 0.6) points in the reciprocal lattice. Some of these scans are shown in Fig. 3 (bottom panel).

After some time, two clearly resolved peaks appear on the sides of the specular peaks. As mentioned before, in this experiment the ion beam impinges on the surface in a nonsymmetrical geometry, as schematically described in the top panel of Fig. 3. From this geometry, we can define two different sides of the ripple structure: one is ''illuminated'' directly by the beam (side I), while the other is in the ''dark'' region of the beam (side D). From the experimental setup, in the scans reported in Fig. 3, bottom panel, we can assign the left peak (with respect to the central Bragg one) to the D side, while the right corresponds to the I side. Already by visual inspection, one can see that the satellite peaks have asymmetric splitting, indicating that the ripple facets are adopting two inequivalent slopes. From the position of the two satellites peaks, we can calculate the local slope ϑ_D, ϑ_I of the facets, since the satellite splitting is linearly dependent on the value of **L** [cf. Fig. 3b in Ref. 13].

Collecting many scans at a typical time interval of 100 sec, we were able to plot the local slope of the facets as a function of sputtering time. The results are presented in Fig. 4 for three different temperatures.

The time evolution of the local slope is dependent on the sputtering temperature. At $T=180$ K (LTR phase) only scans along the *H* direction reveal the presence of a lateral peak. The LTR phase is strongly asymmetric: the ripple side I is very steep at the beginning (about 20°) while for the opposite face the slope is a factor-of 10-lower. Increasing the ion dose, the nanostructure evolves into a more regular shape,

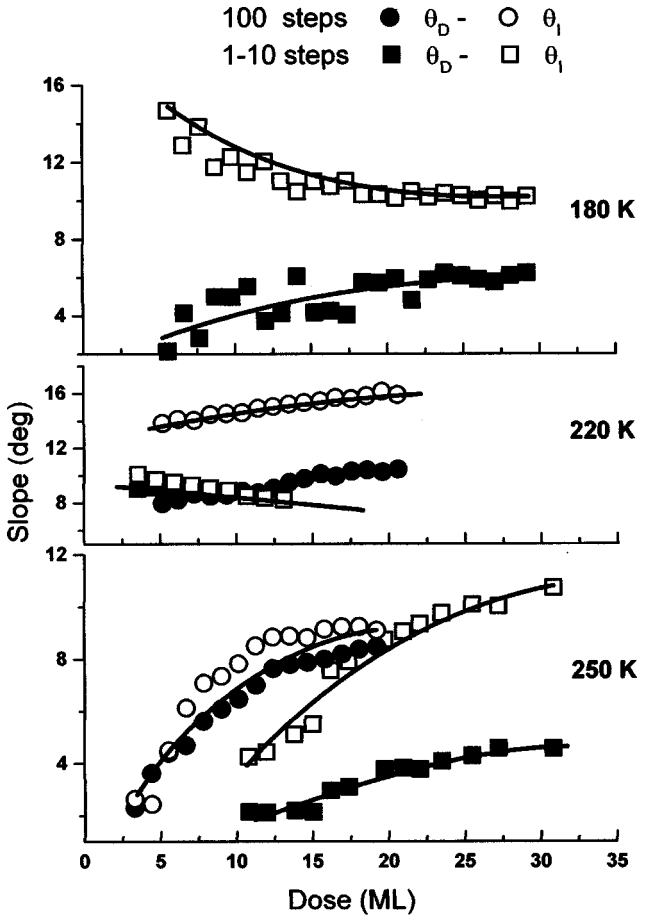

FIG. 4. Evolution of the local facet slope vs ion dose at 180 K, 220 K, and 250 K.

reaching an equilibrium value of about 10° on the I side and 7° on the D side. At $T=220$ K, the ITM phase is present: *H* and *K* scans present well-resolved lateral peaks. In this condition, the situation is drastically changed with respect to LTR: along *K* the slope is almost the same for both sides within experimental error and remains constant in time (slope selection); along *H*, the difference is now about 5° and a slow increase can be observed for both sides. At $T=250$ K, we are again in an ITM condition, but the behavior is changed again: the facets along *K* are equal, but they evolves to gain an equilibrium value of about 9°; the facets along *H* present a difference of about 3° which also remains nearly the same after a long time.

The results presented above show that Cu(110), when sputtered with energetic ions, organizes itself in ordered nanostructures. The observed transition between different phases (LTR→ITM→HTR) is similar to that observed in Ag(110),[13] obviously in a different temperature range since the activation energy for the diffusion processes is different between the two materials. However, the real-time observation of the slope evolution indicates that the nanostructuring process evolves in a complicated way.

The first result is that only after an argon dose of 20–25 ML does the system reache an equilibrium shape, independently of temperature. On the contrary, at the beginning of the sputtering process, a marked anisotropy in the shape of

nanostructures has been observed. Remarkable is the observation that at low temperature, the two sides evolve in opposite directions (cf. Fig. 4). An asymmetry in the shape of a ripple structure has been recently reported by Umbach *et al.*[17] in the case of SiO_2: they fitted the data obtained in GISAXS experiments by using a triangular profile with two different base angles. However, in their model, the steeper side is the D side, contrary to our observations; moreover, the authors do not report on the time evolution of the shape, but only discuss the morphology at equilibrium. In our case, we suggest that the asymmetry is mainly due to the sputtering geometry: in our previous experiments, in which the ion beam was in the x-ray scattering plane, we never observed such an asymmetry. Our hypothesis is that the present geometry unbalances the competition between erosion and diffusion, favoring a different mass transport in the two sides. The effective incident flux on the two facets I and D is different due to the different local slopes: for example, for $\vartheta_D = 5°$ and $\vartheta_I = 10°$ (two typical values for the base angles) and for $\delta = 36°$, it results in $\Phi_I \cong 1.4\Phi_D$ where Φ indicates the ion flux. Since the rate of production of surface defects (vacancy and adatoms) is proportional to the effective flux, a 40% difference is important in the net mass transport on the surface.

Apart from the asymmetry, the other important result is that we observed a constant slope only in a restricted temperature range, around 220 K. Out of this range, the local slope evolves in time for both surface directions, until it reaches an equilibrium value. In other words, we were able to measure the time the system needs to reach the slope selection. Such a behavior must be related to the microscopic processes involved in the sputtering process. We know that ion sputtering produces vacancy and adatom clusters around the ion impact point.[18] In this light, we compare our results with those reported from growth experiments and simulations.

Slope evolution in time has been observed in epitaxial deposition of Cu on Cu(100):[19] the average slope doubles in the range of 1–100 ML of deposited copper. Also, computer simulations[20–22] show a relevant increase in the slope as a function of the deposited material and in Ref. 20 it is also reported that at low temperature the slope can decrease, in qualitative agreement with our result at 180 K. We notice that also a different model, which takes into account the dependence of the Ehrlich-Schwoebel barrier on the terrace size, produces a slope evolution in agreement with the presented results.[27]

Starting from different continuum equations, in recent years many authors investigated the time evolution of ion-sputtered surfaces (or equivalently the time evolution of the growth front in deposition experiments).[23–26] In this approach, the surface morphology is described by a continuum function which changes in time in a complicated way due to the presence of nonlinear terms in the equations. We cannot compare in this paper our results with these models in more detail, but many aspects of our findings (the transition between different phases with temperature and the time evolution of the local slope) are in qualitative agreement with these results.

Finally, we want to emphasize that both in GISAXS and CTR scans the lateral shoulder appears at different times (i.e., doses) for *K* and *H* scans (for example, see Fig. 3). This clearly indicates different times in the self-organization of the surface, probably related to the different energies to create steps along one or other surface direction.

In conclusion, we have demonstrated that Cu(110), bombarded by energetic ions, organizes itself in ordered nanostructures. While the periodicity evolves in time, following a simple power law, the shape changes, gaining an equilibrium form which is temperature dependent. This change is not fully understood, but it is surely related to the microscopic processes of the surface defects (vacancies and adatoms) produced by the ions.

This work was supported by a grant from INFM (PURS project).

[1] E. Chason, T. M. Mayer, B. K. Kellerman, D. T. McIlroy, and A. J. Howard, Phys. Rev. Lett. **72**, 3040 (1994).
[2] J. Erlebacher, M. J. Aziz, E. Chason, M. B. Sinclair, and J. A. Floro, Phys. Rev. Lett. **82**, 2330 (1999).
[3] S. Habenicht, K. P. Lieb, W. Bolse, U. Geyer, F. Roccaforte, and C. Ronning, Nucl. Instrum. Methods Phys. Res. B **161**, 958 (2000).
[4] S. Facsko, T. Dekorsy, C. Koerdt, C. Trappe, H. Kurz, A. Vogt, and H. L. Hartnagel, Science **285**, 1551 (1999).
[5] S. Facsko, T. Bobek, T. Dekorsy, and H. Kurz, Phys. Status Solidi B **224**, 537 (2001).
[6] S. Rusponi, C. Boragno, and U. Valbusa, Phys. Rev. Lett. **78**, 2795 (1997).
[7] T. Michely and G. Comsa, Surf. Sci. **256**, 217 (1991).
[8] R. M. V. Murty, T. Curcic, A. Judy, B. H. Cooper, A. R. Woll, J. D. Brock, S. Kycia, and R. L. Headrick, Phys. Rev. Lett. **80**, 4713 (1998).
[9] S. Rusponi, G. Costantini, F. B. de Mongeot, C. Boragno, and U. V. Valbusa, Appl. Phys. Lett. **75**, 3318 (1999).
[10] M. Ritter, M. Stindtmann, M. Farle, and K. Baberschke, Surf. Sci. **348**, 243 (1996).
[11] H. J. Ernst, Surf. Sci. **383**, L755 (1997).
[12] S. Rusponi, G. Costantini, C. Boragno, and U. Valbusa, Phys. Rev. Lett. **81**, 2735 (1998).
[13] C. Boragno, F. Buatier de Mongeot, G. Costantini, U. Valbusa, R. Felici, and S. Ferrer, Nucl. Instrum. Methods Phys. Res. B **193**, 590 (2002).
[14] M. Rauscher, R. Paniago, H. Metzger, Z. Kovats, J. Domke, J. Peisl, H. D. Pfannes, J. Schulze, and I. Eisele, J. Appl. Phys. **86**, 6763 (1999).
[15] I. K. Robinson and D. J. Tweet, Rep. Prog. Phys. **55**, 599 (1992).
[16] S. Ferrer and F. Comin, Rev. Sci. Instrum. **66**, 1674 (1995).
[17] C. C. Umbach, R. L. Headrick, and Kee-Chul Chang, Phys. Rev. Lett. **87**, 246104 (2001).

[18] G. Costantini, F. Buatier De Mongeot, C. Boragno, and U. Valbusa, Phys. Rev. Lett. **86**, 838 (2001).
[19] J. K. Zuo and J. F. Wendelken, Phys. Rev. Lett. **78**, 2791 (1997).
[20] G. Amar and F. Family, Phys. Rev. B **54**, 14 742 (1996).
[21] P. P. Chatraphorn, Z. Toroczkai, and S. D. Sarma, Phys. Rev. B **64**, 205407 (2001).
[22] F. Hontinfinde, R. Ferrando, and A. C. Levi, Physica A **248**, 288 (1998).
[23] R. Cuerno and A. L. Barabasi, Phys. Rev. Lett. **74**, 4746 (1995).
[24] R. Cuerno, H. A. Makse, S. Tomassone, S. T. Harrington, and H. E. Stanley, Phys. Rev. Lett. **75**, 4464 (1995).
[25] J. T. Drotar, Y.-P. Zhao, T.-M. Lu, and G.-C. Wang, Phys. Rev. E **59**, 177 (1999).
[26] Y. P. Zhao, H. N. Yang, G. C. Wang, and T. M. Lu, Phys. Rev. B **57**, 1922 (1998).
[27] E. Wang (private communication).